

SUPPLEMENTARY NOTES

Data

The isotopic He data used in this study were collected during a series of hydrographic transects (Fig. 1) conducted as part of the World Ocean Circulation Experiment (WOCE) and the U.K. ALBATROSS project in the 1990s. Data from the latter cruise provide the initial and final boundary conditions for our diagnostic of mixing and upwelling rates in the southwest Atlantic, whereas data from the WOCE S3 (an ACC chokepoint transect south of Tasmania, not shown) and P16 sections are used in defining the background tracer distribution in the ACC upstream of the eastern Pacific injection sites. Prior to the calculation, the concentration of non-atmospheric ^3He ($^3\text{He}_{na}$, which for all practical purposes equals the concentration of primordial ^3He in our depth range of interest) is evaluated for all data sets from measured He and Ne parameters using a component separation technique^{33,34}. The uncertainty in $^3\text{He}_{na}$ is $\pm 2.5\%$, a negligible fraction of the signal-to-noise ratio of the tracer-release experiment. This $^3\text{He}_{na}$ variable, available at selected stations and depths only, is objectively mapped to a finer grid involving all the stations in the respective hydrographic transect and 2 dbar pressure intervals. The mapping is performed along surfaces of constant neutral density³¹ γ^n using an optimal estimation algorithm³⁵.

Definition of the control volume of the calculation

The rationale of our definition of the control volume of the calculation is to avoid the intractable complexity introduced by mixing of the ACC waters under study with recently ventilated, ^3He -poor ($^3\text{He}_{na} < 0.3 \text{ fmol kg}^{-1}$) Weddell Sea waters found at the southern edge of the Scotia Sea (Figs. 1 and 3). This interaction is particularly evident in the ACC south of South Georgia, where mixing with Weddell Sea waters reduces $^3\text{He}_{na}$ below values at the same density in Drake Passage. The same effect is apparent below the ^3He plume's core in the Georgia Basin. To avoid the influence of these new end-members, we exclude those parts of the ALBATROSS section affected by Weddell Sea waters from the calculation. Based on a water mass analysis³⁶, we conservatively leave out all layers denser than $\gamma^n = 28.00 \text{ kg m}^{-3}$ and all regions poleward of $\psi = \psi_s = 120 \text{ Sv}$ ($1 \text{ Sv} = 10^6 \text{ m}^3 \text{ s}^{-1}$), where ψ is the full-depth volume transport streamfunction estimated with an inverse model³² (Fig. 3). This streamline lies on the equatorward flank of the Southern ACC Front and marks the boundary between ACC waters flowing north and south of South Georgia.

Calculation of the cross-stream isopycnal tracer spreading $\Delta\sigma_\psi^2$

In order to estimate $\Delta\sigma_\psi^2$, we first define the background tracer concentration ($\langle ^3\text{He}_{na} \rangle$) in the ACC as a sole function of γ^n (Fig. 2), a simplification that represents the ACC $^3\text{He}_{na}$ field in the western and central Pacific accurately. The resulting distribution of [$^3\text{He}_{na} - \langle ^3\text{He}_{na} \rangle$] is characterized by two prominent peaks aligned with the SAF and the northern flank of the PF and separated by a region of low concentration that arises from a northwestward meander of the PF (Fig. 3, upper panel). Since calculating $\Delta\sigma_\psi^2$ using the expression for the lateral diffusion of a Gaussian tracer¹⁵ (our method of choice) requires that the initial tracer distribution approximates to a Gaussian peak, we reorder the stations in Drake Passage according to hydrographic characteristics. This results in a shift of the tracer-poor stations within the PF meander to the region south of the PF and a collapse of the inflowing tracer distribution into a single, thin quasi-Gaussian peak. Then, we calculate σ_ψ^2 for $\int [^3\text{He}_{na} - \langle ^3\text{He}_{na} \rangle] dz$ in Drake Passage and the outflow region, where the column integral is taken over the part of the $^3\text{He}_{na}$ plume ($27.73 < \gamma^n < 28.00 \text{ kg m}^{-3}$) unaffected by mixing with Weddell Sea waters. We evaluate σ_ψ^2 as $(M_2 - M_1^2)/M_0$, with M_n designating the n^{th} lateral moment of the tracer distribution¹⁵. In doing so, we take account of the general divergence of streamlines as the ACC flows through the Scotia Sea by normalizing the width of the ACC equatorward of ψ_s in each of the sections to their average value ($L \approx 1000 \text{ km}$). This implicitly assumes that the width of the ACC increases approximately linearly and that the tracer mixes at a roughly constant rate in crossing the Scotia Sea, as suggested by the steadily divergent climatological fronts (Fig. 1) and rather homogeneous eddy characteristics in the study region¹⁷. The resulting σ_ψ are $42 \pm 15 \text{ km}$ for the inflow and $272 \pm 20 \text{ km}$ for the outflow, yielding $\Delta\sigma_\psi^2 = (7.20 \pm 1.10) \times 10^4 \text{ km}^2$. If the normalization to a common ACC width is abandoned, the downstream broadening of the current increases $\Delta\sigma_\psi^2$ (and hence K_ψ) by a factor of 2.

Note, however, that the above characterization of the cross-stream spreading of the tracer could be affected by the lateral reorganization of streamlines within the Scotia Sea and any existing along-track variability in the angle at which the hydrographic section intersects the ACC, as well as by true cross-stream tracer displacement. Thus, in order to fine-tune our $\Delta\sigma_\psi^2$ estimate, we attempt to isolate the cross-stream tracer displacement through the additional re-scaling of along-section distance

by a monotonic functional approximation to ψ (Fig. 2). The scaling reflects our dynamically based preconception³⁷ that clusters of streamlines at frontal jets act as barriers to the spreading of the tracer, in contrast to regions with weak or recirculating flow where there is little dynamical opposition to tracer displacement. The scaling broadens the inflowing tracer distribution substantially, giving more weight to the tracer-rich SAF and PF jets, and focuses the outflowing tracer distribution slightly around its centre of mass. As a result, σ_ψ increases to $235 \pm 15 \text{ km}$ for the inflow while it decreases to $263 \pm 20 \text{ km}$ for the outflow, yielding a $\Delta\sigma_\psi^2$ estimate of $(1.40 \pm 1.25) \times 10^4 \text{ km}^2$ that is significantly lower than our original value. Physically, we may interpret the new reduced $\Delta\sigma_\psi^2$ and K_ψ values to be characteristic of the frontal jet cores, whereas our cruder original estimates are likely more representative of isopycnal mixing conditions in the control volume as a whole.

Calculation of the transit time Δt

In order to estimate Δt , we determine the average time (188 ± 42 days, the uncertainty being estimated *ad hoc* as half the standard deviation) taken by a suite of 23 PALACE floats to transit through the study region at a nominal depth of 900 m ¹⁶. We use the mean geostrophic shear profile of the ACC in Drake Passage³² to scale this time to 227 ± 42 days at 1210 m , the mean depth of the density layer under consideration. This time scale compares well with an independent Δt estimate of 237 ± 20 days, obtained by dividing the approximate volume of water equatorward of the Southern ACC Front and with density in the range $27.73 < \gamma^n < 28.00 \text{ kg m}^{-3}$ in the Scotia Sea ($6 \times 10^{14} \text{ m}^3$, estimated from a hydrographic climatology³⁸) by the volume transport in the same hydrographic zone ($\psi \leq \psi_s$) and density range ($29.2 \pm 2.4 \text{ Sv}$, calculated from the inverse model³²).

Calculation of the isopycnal upwelling rate w_ψ^*

In order to estimate w_ψ^* , we assume that the eddy-driven upwelling is predominantly oriented along isopycnal surfaces. This implies that the mean slope of isopycnals $s_\rho = w_\psi^* / v_\psi^*$, where v_ψ^* is the cross-stream horizontal velocity associated with the upwelling process⁶. v_ψ^* can be estimated from the measured translation of the tracer's centre of mass in ψ space as $v_\psi^* = (\Delta\psi_{CM} / \psi_s) * L * / \Delta t$, implying the following expression for the isopycnal vertical velocity: $w_\psi^* = \Delta\psi_{CM} * L * s_\rho / (\psi_s * \Delta t)$.

Consistency between the estimated rates of isopycnal mixing (K_ψ) and upwelling (w_ψ^*)

If mesoscale eddies may be assumed to be predominantly adiabatic, residual mean theory⁶ suggests that K_ψ and w_ψ^* are related by the expression $w_\psi^* = \partial(K_\psi * s_\rho) / \partial y$, which can be used to investigate the dynamical consistency between our estimated rates of isopycnal mixing and upwelling. Taking the ACC to be bounded by northern and southern regions of flat isopycnals in which $K_\psi * s_\rho \sim 0$, and applying scaling analysis, we can approximate the above expression by $w_\psi^* \sim 2 * K_\psi * s_\rho / L$. Using $K_\psi \sim 2000 \text{ m}^2 \text{ s}^{-1}$, $s_\rho \sim 10^{-3}$ and $L \sim 1000 \text{ km}$, as may be appropriate for our study region as a whole, we obtain $w_\psi^* \sim 4 \times 10^{-6} \text{ m s}^{-1} \sim 130 \text{ m y}^{-1}$, which is on the low side of, but broadly comparable to, our direct estimate of w_ψ^* . Alternatively, we can use $K_\psi \sim 400 \text{ m}^2 \text{ s}^{-1}$, $s_\rho \sim 2 \times 10^{-3}$ and $L \sim 300 \text{ km}$, which are representative of the narrow SAF and PF regions across which the tracer's centre of mass rises. This yields $w_\psi^* \sim 5 \times 10^{-6} \text{ m s}^{-1} \sim 170 \text{ m y}^{-1}$ and lends further support to the suggestion that our tracer-derived estimates of K_ψ and w_ψ^* are generally compatible.

Calculation of the diapycnal tracer spreading $\Delta\sigma_\rho^2$

In order to estimate $\Delta\sigma_\rho^2$, we could, in principle, calculate the moments of the initial and final tracer profiles directly, in analogy to the evaluation of $\Delta\sigma_\psi^2$. However, this technique yields results that are overly sensitive to the prescribed background tracer distribution. A more robust alternative³⁹ consists of fitting a half-normal distribution in the range $27.73 \leq \gamma^n \leq 27.98 \text{ kg m}^{-3}$ to profiles of $[\int [^3\text{He}_{na} - \langle ^3\text{He}_{na} \rangle] dl / |dl|]$, where dl is a length increment and the integral is now taken along isopycnals for the ACC equatorward of ψ_s . In adopting this approach, we assume that the diapycnal spreading of the tracer is symmetric about the plume axis (i.e., $\partial K_\rho / \partial z \approx 0$ at mid-depth) and, anticipating that diapycnal mixing is widespread in the region¹³, we reference the tracer distribution in each of the sections to their average density profile. σ_ρ^2 then measures the width of the fitted normal distribution. From our initial ($524 \pm 4 \text{ m}$) and final ($536 \pm 7 \text{ m}$) estimates of σ_ρ , we obtain $\Delta\sigma_\rho^2 = (1.27 \pm 0.88) \times 10^4 \text{ m}^2$.

Calculation of the rate of energy conversion by eddies E_{eddy}

The rate at which eddies in the control volume extract energy from the mean flow can be expressed¹⁰ as

$$E_{eddy} = \int g^* s_\rho^* [v^* \rho^*] dz,$$

where the square brackets denote a temporal average over several eddy life cycles and

the integral is taken over the depth H of the control volume. We wish to define E_{eddy} in terms of the isopycnal upwelling rate w_{ψ}^* measured by the spreading of the tracer. This can be related to the meridional eddy density flux using the equation

$$w_{\psi}^* = -s_{\rho}^* \partial ([v^* \rho] / (\partial \rho / \partial z)) / \partial z.$$

Assuming that the stratification¹³ and upwelling rate are approximately constant over the control volume and integrating vertically, we obtain:

$$\langle [v^* \rho] \rangle \approx -w_{\psi}^* s_{\rho}^* \partial \rho / \partial z^* H,$$

where the angled brackets indicate an approximate vertical average over the control volume (this supposes that $[v^* \rho]$ decays to small values at the base of the volume, as observed with current meters⁴⁰). Replacing $[v^* \rho]$ in the expression for E_{eddy} by $\langle [v^* \rho] \rangle$, we find:

$$E_{\text{eddy}} \approx -\int g^* w_{\psi}^* \partial \rho / \partial z^* H^* dz.$$

Applying the definition of N^2 and integrating vertically, it follows that

$$E_{\text{eddy}} \approx \rho^* w_{\psi}^* N^2 H^2 \Delta \psi_{\text{CM}} / \psi_s,$$

where the factor $\Delta \psi_{\text{CM}} / \psi_s$ accounts for the fact that the upwelling occurs over a fraction of the width of the control volume. Using $\rho = 1030 \text{ kg m}^{-3}$, $w_{\psi}^* \approx 10^{-5} \text{ m s}^{-1}$, $N^2 \approx 3 \times 10^{-6} \text{ s}^{-2}$, $H \approx 1000 \text{ m}$, $\Delta \psi_{\text{CM}} \approx 40 \text{ Sv}$ and $\psi_s = 120 \text{ Sv}$, we obtain $E_{\text{eddy}} \approx 10 \text{ mW m}^{-2}$. This value is likely to be an underestimate of the total available potential energy conversion in the study region, as eddies also extract energy from the mean flow in density classes outside the control volume.

Error analysis

Errors in $\Delta \sigma_{\psi}$ and K_{ψ}

The random error in σ_{ψ} combines two roughly equally contributing sources of uncertainty: the formal objective mapping error³⁵, which we estimate assuming that the variance statistics of the ${}^3\text{He}_{\text{na}}$ field are well represented by those of the finely resolved CTD oxygen; and the possibility of an offset or a cross-stream trend in the background tracer concentration, which we estimate by reference to the misfits between the western and central Pacific ${}^3\text{He}_{\text{na}}$ distribution and the smoothing spline fit in Figure 2. No explicit account is made of the likely departure of the lateral statistics of the tracer plume from a Gaussian model, which may be an additional significant contribution to the error in σ_{ψ} ¹⁵. The error introduced by the uncertainty in ψ (which largely enters the calculation via the normalization to a common ACC width) is comparatively small. It is reassuring that the combination of the objectively estimated ${}^3\text{He}_{\text{na}}$ with the inverse model velocity field approximately conserves ${}^3\text{He}_{\text{na}}$ in the region, both in a net sense (to within 6% of the full-depth tracer transport through Drake Passage) and in the γ^n and ψ ranges entering the calculation of $\Delta \sigma \psi^2$ (to within 11% of the tracer transport through Drake Passage in those ranges). The underlying small loss of tracer to the ACC south of ψ_s , the upper ocean and the atmosphere likely biases our estimates of $\Delta \sigma \psi^2$ and K_{ψ} low, as does the limitation of the northward spreading of the tracer by the continental slope of South America. Additionally, straining of the tracer distribution associated with the banded nature of the ACC flow may compress the tracer in the cross-stream direction and lead to further underestimation of $\Delta \sigma \psi^2$ and K_{ψ} . We have assessed the size of these biases using a 2-D kinematic advection-diffusion model of the tracer's cross- and along-stream spreading on isopycnals in the presence of an impermeable northern boundary (Supp. Fig. 1). The model is initialized with the observed inflowing depth-integrated tracer distribution in ψ space (normalized to L) and run over a period Δt with K_{ψ} values in the range 200–1500 $\text{m}^2 \text{ s}^{-1}$ and a two-jet flow field that mimics the structure of the ACC in Drake Passage and has a mean speed of $D / \Delta t = 7.6 \times 10^{-2} \text{ m s}^{-1}$, where $D \approx 1500 \text{ km}$ is the approximate along-stream distance between Drake Passage and the outflow region. The results of these sensitivity tests are to some extent dependent on the details of the prescribed flow field, of which we have only a broad knowledge. On the whole, they suggest that our estimates of $\Delta \sigma \psi^2$ and K_{ψ} may be too low by up to ~90%, with the presence of the northern continental boundary introducing by far the largest bias.

Our implicit assumption that the observed tracer distribution is steady to a good approximation is supported by a second estimate of σ_{ψ} in Drake Passage using WOCE A21 data from 1990⁷, nine years before the ALBATROSS cruise, yielding a value (249

$\pm 23 \text{ km}$, obtained by re-scaling along-section distance by a monotonic functional approximation to the baroclinic streamfunction) that is statistically indistinguishable from the result of our original calculation ($235 \pm 15 \text{ km}$). The steadiness of the oxygen concentration (whose mid-depth minimum derives from subtropical Pacific sources, similarly to the mid-depth ${}^3\text{He}_{\text{na}}$ maximum) as a function of baroclinic streamfunction and depth in five Drake Passage transects dating back to 1975 (not shown) further reinforces this assumption. Finally, the error in the mean ACC width (estimated *ad hoc* as $\pm 235 \text{ km}$, one quarter of the difference between the inflow and outflow current widths) results in a rescaling of $\Delta \sigma \psi^2$, K_{ψ} and their uncertainties by a factor of 0.6–1.5.

Errors in $\Delta \sigma$ and K_{ρ}

The random error in σ_{ρ} arises primarily from the uncertainty in the background tracer concentration and, to a lesser extent, from the formal objective mapping error. In order to minimize the impact of the uncertainty in the background concentration, we estimate σ_{ρ} using a weighted least squares fitting procedure that downweights misfits in the upper part of the plume, where the background concentration varies most rapidly with height. The error in σ_{ρ} is then gauged by reference to the uncertainty in the gradient of the background concentration with height above the plume axis. No account is made of the likely departure of the tracer plume statistics from a Gaussian model, which may be an additional significant contribution to the uncertainty in σ_{ρ} ¹⁵. The biases arising from differential horizontal and vertical advection and the assumption of negligible $\partial K_{\rho} / \partial z$ are investigated with a 2-D (along-stream direction vs. depth) kinematic advection-diffusion model of the plume incorporating a vertical shear of up to $3 \times 10^{-5} \text{ s}^{-1}$ ³², $\partial K_{\rho} / \partial z \leq 3 \times 10^{-7} \text{ m s}^{-1}$ ¹³ and $\partial w_{\rho} / \partial z \leq 5 \times 10^{-10} \text{ m s}^{-1}$ thought to be characteristic of the control layer. The model simulations indicate that only horizontal advection has the potential to lead to significant (order 1) under- or overestimation of $\Delta \sigma_{\rho}^2$ and K_{ρ} by distorting the broadening of the tracer peak due to diapycnal mixing. The complexity of tracer spreading in a current of steep isopycnals and large horizontal and vertical shears prevents us from ascertaining whether horizontal advection effects may be biasing our estimates of $\Delta \sigma_{\rho}^2$ and K_{ρ} substantially. Nonetheless, it is reassuring that a diapycnal shoaling of the tracer peak (which is intrinsic to all the simulations in which $\Delta \sigma_{\rho}^2$ and K_{ρ} are overestimated) is absent from our observations (Fig. 2), suggesting that significant overestimation of those variables is unlikely.

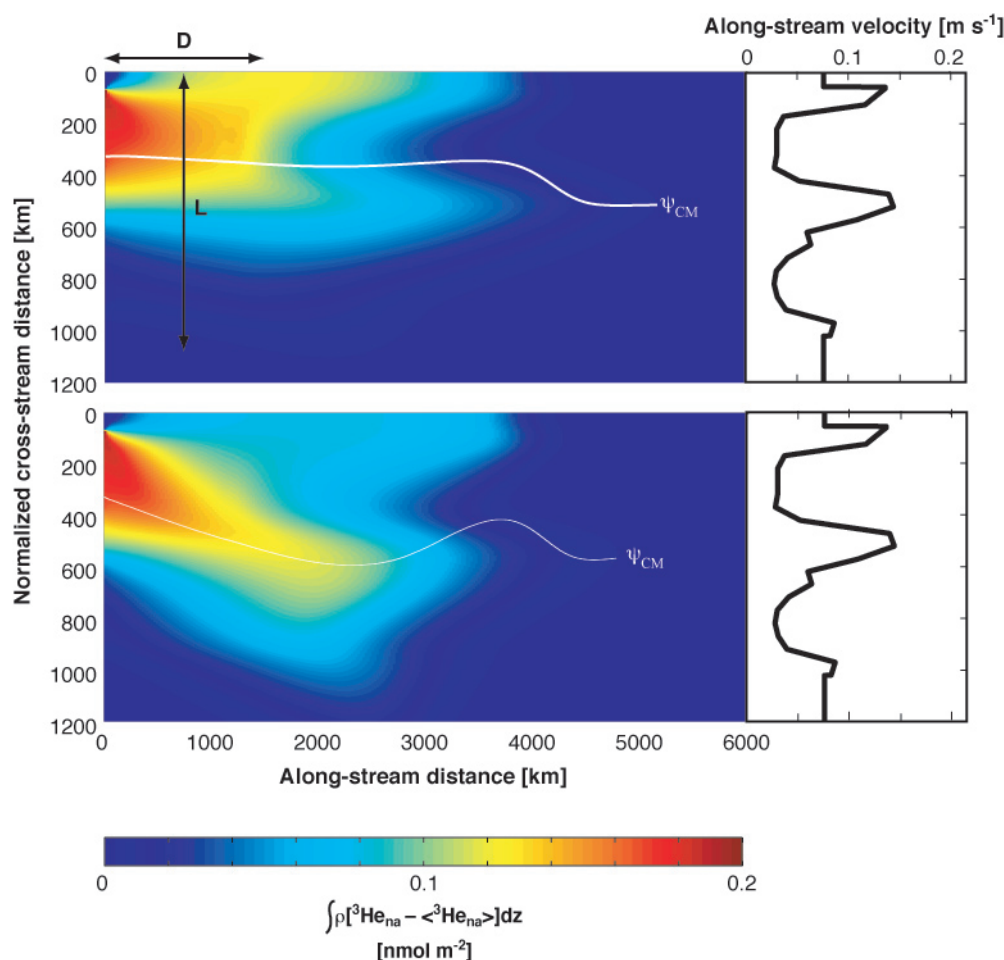
As was the case with σ_{ψ} , our assumption of steadiness is supported by the unchanging structure of the mid-depth oxygen minimum in Drake Passage and a calculation of σ_{ρ} using WOCE A21 data, which yields a value ($522 \pm 5 \text{ m}$) that is comparable to our original estimate. Lastly, the error in the mean height of γ^n surfaces introduces a negligible uncertainty in σ_{ρ} and K_{ρ} .

Error in w_{ψ}^*

The error in w_{ψ}^* stems principally from two factors: the uncertainty in $\Delta \psi_{\text{CM}}$, which we estimate as $\pm 10 \text{ Sv}$ from the error in ψ (Fig. 3); and the presence of a continental boundary to the north of the ACC, which skews the translation of the tracer's centre of mass poleward. This bias is evaluated with the same 2-D advection-diffusion model used to assess the robustness of our $\Delta \sigma_{\psi}^2$ and K_{ψ} estimates (Supp. Fig. 1). Experiments with an identical range of K_{ψ} values suggest that w_{ψ}^* may be overestimated by up to 20%, and it is reassuring that obtaining a purely diffusive cross-stream translation of the tracer's centre of mass of the measured magnitude requires the model to be run with unphysically high K_{ψ} values of $\sim 10^4 \text{ m}^2 \text{ s}^{-1}$. Regardless, evidence in support of our diagnosed UCDW upwelling rate is provided by the along-stream change in the layer's volume transport as the ACC crosses the study region³². This change implies a poleward cross-stream UCDW transport (T_{UCDW}) of 8 Sv distributed over a depth range H and an along-stream distance D , yielding $w_{\psi}^* \sim T_{\text{UCDW}} s_{\rho} / (H^* D) \sim 5 \times 10^{-6} \text{ m s}^{-1} \sim 170 \text{ m } \gamma^{-1}$, i.e. within a factor of 2 of our tracer-derived estimate. The rate of energy transfer from the ACC mean flow to its eddy field implied by our w_{ψ}^* estimate is broadly compatible with localised measurements of the energy conversion rate from current meters moored in Drake Passage⁴⁰, which suggest an upper limit of $E_{\text{eddy}} \sim 40 \text{ mW m}^{-2}$ there when extrapolated to the entire water column.

33. Roether, W., Well, R., Putzka, A. & R uth, C. Component separation of oceanic helium. *J. Geophys. Res.* **103**, 27931–27946 (1998).
34. Roether, W., Well, R., Putzka, A. & R uth, C. Correction to ‘‘Component separation of oceanic helium’’. *J. Geophys. Res.* **106**, 4679 (2001).
35. Roemmich, D. Optimal estimation of hydrographic station data and derived fields. *J. Phys. Oceanogr.* **13**, 1544–1545 (1983).
36. Naveira Garabato, A. C., Heywood, K. J. & Stevens, D. P. Modification and pathways of Southern Ocean deep waters in the Scotia Sea. *Deep-Sea Res.* **149**, 681–705 (2002).
37. Samelson, R. M. Fluid exchange across a meandering jet. *J. Phys. Oceanogr.* **22**, 431–440

- (1992)
38. Orsi, A. H. & Whitworth III, T. Hydrographic Atlas of the World Ocean Circulation Experiment (WOCE). Volume 1: Southern Ocean (eds. Sparrow, M., Chapman, P. & Gould, J.), International WOCE Project Office, Southampton, U.K. (2004).
39. Law, C. S., Abraham, E. R., Watson, A. J. & Liddicoat, M. I. Vertical eddy diffusion and nutrient supply to the surface mixed layer of the Antarctic Circumpolar Current. *J. Geophys. Res.* **108**, 3272, doi:10.1029/2002JC001604 (2003).
40. Bryden, H. L., Poleward heat flux and conversion of available potential energy in Drake Passage. *J. Mar. Res.* **37**, 1–22 (1979).



Supplementary Figure 1. Illustration of results from a 2-D kinematic advection-diffusion model of the tracer spreading along and across ACC streamlines, run for 1 year. Colour shows tracer concentration relative to background levels. Cross-stream distance is indicated by the full-depth volume transport streamfunction ψ scaled by L/ψ_s , where $L \approx 1000$ km is the mean width of the control zone of the ACC in the study region and $\psi_s = 120$ Sv is the streamfunction coordinate of the southern boundary of the control zone. North is on the upper axis. The figures correspond to simulations with $K_\psi = 1000$ m² s⁻¹ and either $w_\psi^* = 0$ (above) or $w_\psi^* = 10^{-5}$ m s⁻¹ (below). The prescribed along-stream velocity is shown in the right-hand panels and largely corresponds to the mean velocity in the control layer in Drake Passage as a function of ψ , with small velocity reversals introduced manually at sites of measured local westward flow and a small scaling applied to make the velocity averaged over L equal to $D/\Delta t = 7.6 \times 10^{-2}$ m s⁻¹. The white lines labelled ψ_{CM} mark the position of the centre of mass of the

tracer in the cross-stream direction, which deviates little from its initial value for $w_\psi^* = 0$ but suggests that the tracer's centre of mass near a distance $D \approx 1500$ km from the origin is displaced southward by $\sim L/4$ for $w_\psi^* = 10^{-5}$ m s⁻¹, close to the observed value ($\sim L/3$). Note that the presence of a solid northern boundary induces an accumulation of tracer in the northern rim of the model domain that would not occur otherwise. This is particularly noticeable for $w_\psi^* = 0$. For $w_\psi^* = 10^{-5}$ m s⁻¹, the tracer distribution near a distance D from the origin is reminiscent of observations at the outflow of the control region (Fig. 3). In this case, the model reproduces a smooth, reversing meridional gradient in tracer concentration of realistic magnitude ($\sim 10^{-4}$ nmol m⁻² km⁻¹) and a faint maximum broadly aligned with $L/2$, on the northern flank of the PF jet. This general compatibility with observations suggests that the model is adequate for assessing biases in our estimates of K_ψ and w_ψ^* brought about mainly by the presence of the South American landmass at the northern edge of the control layer.